Inexact yet Accurate: Unlocking low precision for efficient quantum modelling of materials at scale

Phani Motamarri, Assistant Professor
Materials-physics & Algorithmic Techniques Research In eXtreme-computing (MATRIX) Lab
Department of Computational and Data Sciences (CDS)
Indian Institute of Science (IISc), Bangalore, India

Joint work with PhD students

Quantum modeling of materials: Impact on Science

Citations of seminal work of Walter Kohn (1964,1965) [Nobel Prize in Chemistry: 1998]

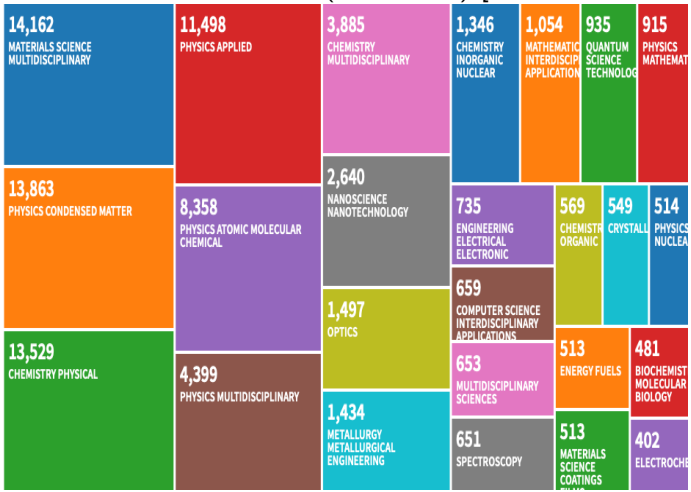

12 of the 100 most-cited papers pertain to Kohn-Sham density functional theory (DFT)

(Nature,**514**, 550 (2014))

Kohn-Sham Density Functional Theory (DFT) : Nonlinear eigenproblem

Many-body Schrödinger equation (Interacting electron problem)

$$\mathbf{H}\Psi = E\Psi$$

$$\mathbf{H} := -\frac{1}{2}\sum_{i}^{N_e}\nabla_i^2 - \frac{1}{2}\sum_{I}^{N_a}\frac{1}{m_I}\nabla_I^2 - \sum_{i}^{n_e}\sum_{I}^{N_a}\frac{Z_I}{|\mathbf{r}_i - \mathbf{R}_I|} + \frac{1}{2}\sum_{\substack{i,j=1\\ i\neq j}}^{N_e}\frac{1}{|\mathbf{r}_i - \mathbf{r}_j|} + \frac{1}{2}\sum_{\substack{I,J=1\\ I\neq J}}^{N_a}\frac{1}{|\mathbf{R}_I - \mathbf{R}_J|}$$

$\Psi(\mathbf{r}_1, \mathbf{r}_2 ..., \mathbf{r}_{N_e}, \mathbf{R}_1, \mathbf{R}_2, ..., \mathbf{R}_{N_a}), \Psi : \mathbb{R}^{3N_e} \rightarrow \mathbb{C}$ **(Exponential complexity)**

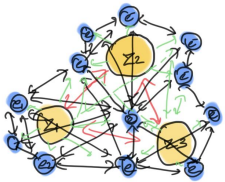

DFT Non-interacting problem

$$E\left[\{\psi_n\}, \mathbf{R}\right] = \mathsf{T}_s + E_{\text{xc}}[\rho] + E_{\text{ext}}\left[\rho, \mathbf{R}\right] + E_{\text{H}}\left[\rho\right] + E_{\text{ZZ}}$$

subject to: $\int \psi_n^*(\mathbf{x})\psi_m(\mathbf{x})d\mathbf{x} = \delta_{nm}$

$$\mathsf{T}_s\left[\{\psi_n\}\right] := f_n \int \psi_n^*(\mathbf{x})(-\frac{1}{2}\nabla^2)\psi_n(\mathbf{x})d\mathbf{x}$$

$$E_{\text{H}}\left[\rho\right] := \int\int \frac{\rho(\mathbf{x})\rho(\mathbf{x}')}{|\mathbf{x} - \mathbf{x}'|}d\mathbf{x}d\mathbf{x}'$$

$$E_{\text{ext}}\left[\rho\right] := \int \rho(\mathbf{x})V_{\text{ext}}(\mathbf{x})d\mathbf{x}$$

DFT eigenvalue problem

$$\left(-\frac{1}{2}\nabla^2 + V_{\text{eff}}(\rho)\right)\psi_n = \varepsilon_n\psi_n$$

$$\rho(\mathbf{x}) = \sum_n f_n|\psi_n(\mathbf{x})|^2$$

$$\sum_n f_n = N_e, \quad \psi_n : \mathbb{R}^3 \rightarrow \mathbb{C}$$

$n = 1 \cdots N_e$ (Smallest eigenpairs)

(Cubic complexity)

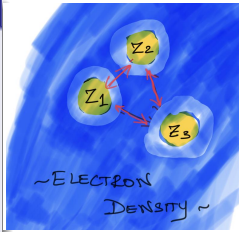

Governing equations in DFT [Projector-augmented wave (PAW) formalism]

Nonlinear generalised eigenvalue problem (Self-consistent field iteration)

$$\left(-\frac{1}{2}\nabla^2 + V_{\text{eff}}(\widetilde{n}) + H_{\text{nl}}\right)\widetilde{\psi}_n = \epsilon_n \left(I + S_{\text{nl}}\right)\widetilde{\psi}_n \quad \text{for} \quad n = 1, \cdots N$$

$$\begin{aligned}
\widetilde{n}(\mathbf{x}) &= 2\sum_n f_n |\widetilde{\psi}_n(\mathbf{x})|^2; \\
\widetilde{b}(\mathbf{x}) &= \sum_a \left(\Delta^a_0 g^a(\mathbf{x}) + \sum_{lm}\sum_{\alpha\beta} \Delta^a_{\alpha\beta,lm} D^a_{\alpha\beta} g^a_{lm}(\mathbf{x}) \right) \\
f(\epsilon_n, \mu) &= 1/[1 + \exp((\epsilon_n - \mu)/k_B\, T)]
\end{aligned}$$

$$-\nabla^2 \phi(\mathbf{x}) = 4\pi(\widetilde{n}(\mathbf{x}) + \widetilde{b}(\mathbf{x}, \mathbf{R}))$$

$$V_{\text{eff}} = {}^{\delta E_{\text{xc}}}/_{\delta \widetilde{n}} + \phi(\mathbf{x})$$

$$H_{\text{nl}} = \sum_a \sum_{\alpha\beta} |p^a_\alpha\rangle\, h^a_{\alpha\beta}\, \langle p^a_\beta|, \; S_{\text{nl}} = \sum_a \sum_{\alpha\beta} |p^a_\alpha\rangle\, \Delta^a_{\alpha\beta 0}\, \langle p^a_\beta|$$

Numerical discretization of governing equations: Finite-element basis

Advantages of finite-element basis

- Real space → accommodates fully periodic, semi-periodic and fully non-periodic boundary conditions.
- Piecewise continuous (C^0) polynomial basis → systematic convergent behaviour.
- Compact support of basis → amenable for large-scale parallelization on multi-CPU and multi-GPU architectures.
- Adaptive resolution → reducing computational cost.

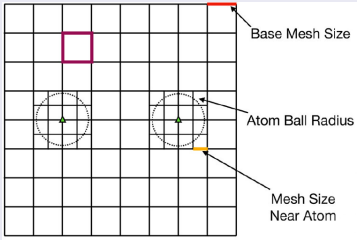

FE discretized sparse nonlinear eigenproblem

Finite-element approximation of electronic fields $\widetilde{\psi}_i^h(\boldsymbol{x}) = \sum_J^G N_J(\boldsymbol{x})\widetilde{\psi}_i^J, \quad \phi^h(\boldsymbol{x}) = \sum_J^G N_J(\boldsymbol{x})\phi^J$

gives rise to the generalized eigenproblem $\mathbf{H}\tilde{\psi}_i = \epsilon_i^h \mathbf{S}\tilde{\psi}_i$ for $i = 1..N$ (N is proportional to N_e)

Numerical discretization of governing equations: Finite-element basis

FE discretized Hamiltonian (**H**) and the Overlap matrix (**S**) in the eigenproblem

$$\mathrm{H}_{JK} = \int \left(\frac{1}{2} \nabla N_J(\boldsymbol{x}) \cdot \nabla N_K(\boldsymbol{x}) + V^h_{\text{eff}}(\mathbf{x}) N_J(\boldsymbol{x}) N_K(\boldsymbol{x}) \right) d\boldsymbol{x} + \sum_{a, i_1 i_2} \int N_J(\boldsymbol{x}') p^a_{i_1}(\boldsymbol{x}') d\boldsymbol{x}' h^a_{i_1 i_2} \int N_K(\boldsymbol{x}) p^a_{i_2}(\boldsymbol{x}) d\boldsymbol{x}$$

$$\mathrm{S}_{JK} = \int N_J(\boldsymbol{x}) N_K(\boldsymbol{x}) d\boldsymbol{x} + \sum_a \sum_{i_1 i_2} \int N_J(\boldsymbol{x}') p^a_{i_1}(\boldsymbol{x}') d\boldsymbol{x}' \sqrt{4\pi} \Delta^a_{i_1 i_2 0} \int N_K(\boldsymbol{x}) p^a_{i_2}(\boldsymbol{x}) d\boldsymbol{x}$$

$$\text{with } h^a_{i_1 i_2} = \left[\sum_{l,m} \Delta^a_{i_1 i_2 L} \int g^a_{l,m}(\boldsymbol{y}) \phi^h(\boldsymbol{y}) d\boldsymbol{y} + \Delta T^a_{i_1 i_2} + \Delta C^a_{i_1 i_2} + 2 \sum_{i_3 i_4} D^a_{i_3 i_4} * \Delta C^a_{i_1 i_2 kl} + \frac{\delta \Delta E^a_{xc}}{\delta D^a_{i_1 i_2}} \right]$$

The matrix represenation for $\mathbf{S}$ is given as $\mathbf{S} = \mathbf{M} + \mathbf{P} \mathbf{\Delta}_s \mathbf{P}^T$

FE discretized Poisson equation for total electrostatic potential

$$\sum_{J=1}^{G} \left(\int \nabla N_I(\mathbf{x}) \cdot \nabla N_J(\mathbf{x}) d\mathbf{x} \right) \phi^J = 4\pi \int \left(\tilde{n}(\mathbf{x}) + \tilde{b}(\mathbf{x}) \right) N_I(\mathbf{x}) d\mathbf{x}$$

Chebyshev Filtered Subspace Iteration (ChFSI) for eigenproblem

- Generalized eigenproblem: $\mathbf{H}\tilde{\psi}_i = \epsilon_i^h \mathbf{S}\tilde{\psi}_i$ ($\mathbf{H}, \mathbf{S}$ are $G \times G$ sparse matrices; $G \approx 10^6 - 10^8$; Number of smallest eigenpairs $N \approx 100 - 100,000$)
- Standard eigenproblem: $\widehat{\mathbf{H}}\tilde{\psi}_i = \epsilon_i^h \tilde{\psi}_i$, where $\widehat{\mathbf{H}} = \mathbf{S}^{-1}\mathbf{H}$;
  - Subspace construction (Filtering): $\mathbf{X}_p = T_p(\widehat{\mathbf{H}})\mathbf{X}_0 \implies \mathbf{X}_{k+1}^{(i)} = \alpha \mathbf{S}^{-1}\mathbf{H}\mathbf{X}_k^{(i)} + \beta \mathbf{X}_k^{(i)} + \gamma \mathbf{X}_{k-1}^{(i)}$
  - Rayleigh-Ritz step: $\mathbf{X}_p^\dagger \mathbf{H} \mathbf{X}_p \mathbf{Q} = \mathbf{X}_p^\dagger \mathbf{S} \mathbf{X}_p \mathbf{Q} \mathbf{\Lambda}, \quad \mathbf{X}_F = \mathbf{X}_p \mathbf{Q}$

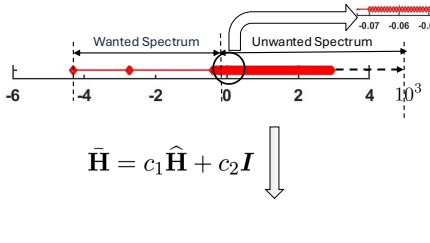

Chebyshev Filtering: $T_m(\bar{\mathbf{H}})\tilde{\mathbf{\Psi}} = \tilde{\mathbf{\Psi}}_F$

$T_m(\bar{\mathbf{H}})\mathbf{X} - [2\bar{\mathbf{H}}T_{m-1}(\bar{\mathbf{H}}) - T_{m-2}(\bar{\mathbf{H}})]\mathbf{X}$

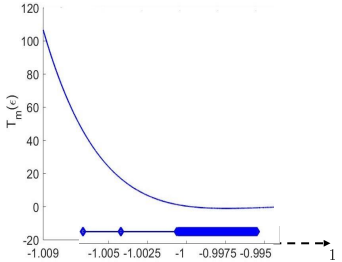

ChFSI: What if filtering is approximate?

$$\mathbf{X}_p = T_p(\mathbf{S}^{-1}\mathbf{H})\mathbf{X}_0 \implies \mathbf{X}_{k+1}^{(i)} = \alpha\mathbf{S}^{-1}\mathbf{H}\mathbf{X}_k^{(i)} + \beta\mathbf{X}_k^{(i)} + \gamma\mathbf{X}_{k-1}^{(i)} \text{ with } k = 1 \cdots p$$

Computing $\mathbf{S}^{-1}$, a $G \times G$ matrix

The overlap matrix: $\mathbf{S} = \mathbf{M} + \mathbf{P}\boldsymbol{\Delta}_s\mathbf{P}^T$ a sparse matrix needs to be inverted.

$$\mathbf{S}^{-1} = \mathbf{M}^{-1} - \mathbf{M}^{-1}\mathbf{P}\left(\boldsymbol{\Delta}_s^{-1} + \mathbf{P}^T\mathbf{M}^{-1}\mathbf{P}\right)^{-1}\mathbf{P}^T\mathbf{M}^{-1} \quad \text{(using the Woodbury identity.)}$$

Suffices to invert a smaller dimension $\left(\boldsymbol{\Delta}_s^{-1} + \mathbf{P}^T\mathbf{M}^{-1}\mathbf{P}\right)$ matrix compared to $G \times G$.

Approximating $\mathbf{S}^{-1}$

- Row-sum lumping approach is used to approximate $\mathbf{M} = \int N_i(\mathbf{x})N_j(\mathbf{x})\,d\mathbf{x}$ as diagonal matrix $\boldsymbol{D}$ and hence inverse of $\mathbf{M}$ to be $\mathbf{D}^{-1}$.
- $\left(\boldsymbol{\Delta}_s^{-1} + \mathbf{P}^T\mathbf{M}^{-1}\mathbf{P}\right)$ is close to block diagonal and approximated as block diagonal.

Consequence of approximate filtering: Stagnation of eigenproblem residual

$$\mathbf{X}_{k+1}^{(i)} = \alpha \mathbf{S}_{apprx}^{-1} \mathbf{H} \mathbf{X}_k^{(i)} + \beta \mathbf{X}_k^{(i)} + \gamma \mathbf{X}_{k-1}^{(i)}$$

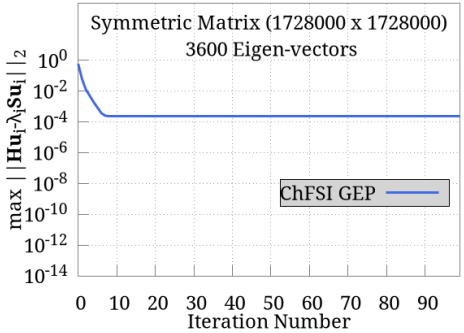

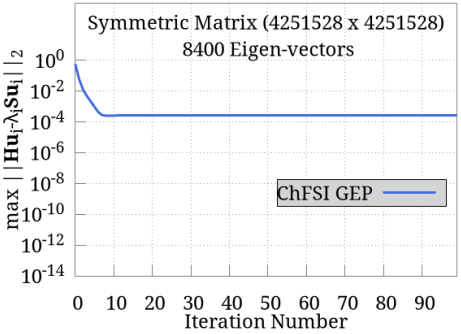

The stagnation of residuals are also observed even when approximations in the form of low-precision arithmetic are employed in evaluating $\mathbf{S}_{apprx}^{-1}\mathbf{HX}$

Proposed remedy: Residual-based Chebyshev filtered subspace iteration (R-ChFSI) [N. Kodali, K. Ramakrishnan, P. Motamarri: Comput. Phys. Commun 2026]

Generalized eigenvalue problem: $\mathbf{H}\tilde{\psi}_i = \epsilon_i^h \mathbf{S}\tilde{\psi}_i \Rightarrow \widehat{\mathbf{H}}\tilde{\psi}_i = \epsilon_i^h \tilde{\psi}_i$, where $\widehat{\mathbf{H}} = \mathbf{S}^{-1}\mathbf{H}$;

1. **Initialization:** Guess for the eigenvector matrix $\mathbf{X}_0$ and the eigenvalues $\mathbf{\Lambda}_0$.
   Define $\mathbf{\Lambda}_k = T_k(\mathbf{\Lambda}_0)/T_k(a_L) = C_k(\mathbf{\Lambda}_0)$.
2. **Subspace construction:** $\mathbf{Y}_k = \mathbf{S}\mathbf{R}_k = \mathbf{S}[C_k(\widehat{\mathbf{H}})\mathbf{X}_0 - \mathbf{X}_0 C_k(\mathbf{\Lambda}_0)]$ and $\mathbf{R} = \mathbf{H}\mathbf{X}_0 - \mathbf{S}\mathbf{X}_0\mathbf{\Lambda}_0$

   $$\mathbf{Y}_{k+1} = \frac{2\sigma_{k+1}}{e}\mathbf{H}\mathbf{S}^{-1}\mathbf{Y}_k - \frac{2\sigma_{k+1}c}{e}\mathbf{Y}_k - \sigma_k\sigma_{k+1}\mathbf{Y}_{k-1} + \frac{2\sigma_{k+1}}{e}\mathbf{R}\mathbf{\Lambda}_k$$

   for $k = 1..p$ where p is Chebyshev polynomial filter degree used for subspace construction.
   Filtered subspace is obtained as $\mathbf{X}_F = \mathbf{X}_p = \mathbf{S}^{-1}\mathbf{Y}_p + \mathbf{X}_0\mathbf{\Lambda}_p$
3. **Rayleigh-Ritz** step to compute approximate eigenvectors:
   (i)Project the Hamiltonian($\mathbf{H}$), and PAW overlap($\mathbf{S}$) onto the subspace as:
   $\mathbf{H}^{\text{proj}} = {\mathbf{X}_F}^T\mathbf{H}\mathbf{X}_F$ and $\mathbf{S}^{\text{proj}} = {\mathbf{X}_F}^T\mathbf{S}\mathbf{X}_F$
   (ii) Solve the generalized eigenvalue problem in the subspace: $\mathbf{H}^{\text{proj}}\boldsymbol{Q} = \mathbf{S}^{\text{proj}}\boldsymbol{Q}\mathbf{\Lambda}$
   (iii) Subspace rotation to obtain the approximate eigenvectors of $\mathbf{H}$: $\widetilde{\mathbf{X}} = \mathbf{X}_F\boldsymbol{Q}$

R-ChFSI vs ChFSI using approximate overlap matrix inverse ($\mathbf{S}^{-1}_{\text{apprx}}$)

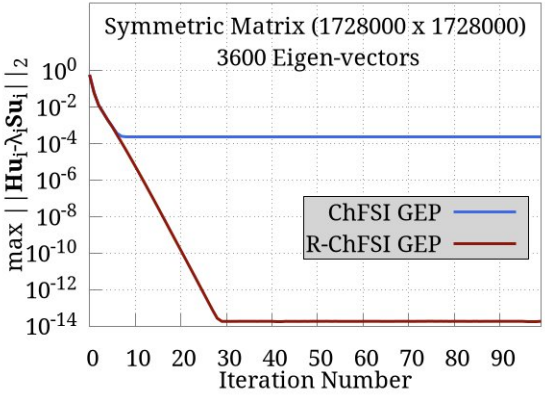

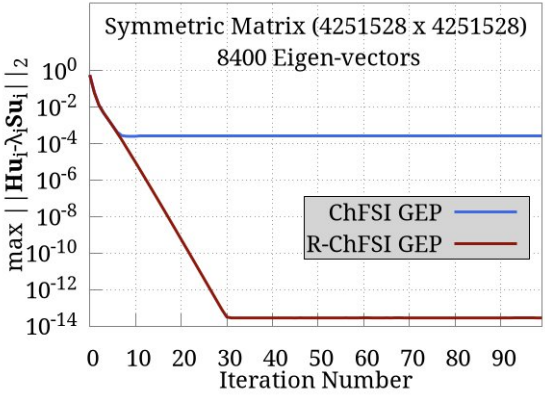

$$\mathbf{Y}^{(i)}_{k+1} = \alpha \mathbf{H}\mathbf{S}^{-1}_{apprx}\mathbf{Y}^{(i)}_{k} + \beta\mathbf{Y}^{(i)}_{k} + \gamma\mathbf{Y}^{(i)}_{k-1}$$

Convergence guarantees of ChFSI and the proposed R-ChFSI

- For an n-dimensional space $\mathcal{S}^{(i)}$ satisfying $\mathcal{S}^{(i)} \cap \mathcal{S}_\perp = \{0\}$ where $\mathcal{S}_\perp$ is the orthogonal complement of the wanted eigenspace $\mathcal{S}$ and $\underline{\mathcal{S}}^{(i+1)} = range\left(\underline{C_p(\widehat{\mathbf{H}})\mathbf{X}^{(i)}}\right)$ with $\mathbf{\Delta}_p^{(i)} = \underline{C_p(\widehat{\mathbf{H}})\mathbf{X}^{(i)}} - C_p(\widehat{\mathbf{H}})\mathbf{X}^{(i)}$ we can write

$$\tan\angle(\underline{\mathcal{S}}^{(i+1)}, \mathcal{S}) \leqslant \left(\frac{|C_p(\lambda_{n+1})| + \left\|\mathbf{\Delta}_p^{(i)}\right\| \csc\angle(\mathcal{S}^{(i)}, \mathcal{S})}{|C_p(\lambda_n)| - \left\|\mathbf{\Delta}_p^{(i)}\right\| \sec\angle(\mathcal{S}^{(i)}, \mathcal{S})}\right) \tan\angle(\mathcal{S}^{(i)}, \mathcal{S})$$

- For convergence, we need

$$|C_p(\lambda_n)| - |C_p(\lambda_{n+1})| > \left\|\mathbf{\Delta}_p^{(i)}\right\| \left(\sec\angle(\mathcal{S}^{(i)}, \mathcal{S}) + \csc\angle(\mathcal{S}^{(i)}, \mathcal{S})\right)$$

- For ChFSI: $\left\|\mathbf{\Delta}_p^{(i)}\right\|$ is nearly constant as i increases $\implies$ the inequality does not hold for all i.
- For R-ChFSI: $\left\|\mathbf{\Delta}_p^{(i)}\right\| \propto \sin\angle(\mathcal{S}^{(i)}, \mathcal{S})$ $\implies$ the inequality can hold for all i.

N. Kodali, K. Ramakrishnan, P. Motamarri: Residual-based Chebyshev filtered subspace iteration for Hermitian eigenvalue problems tolerant to approximate matrix-vector products (accepted in Comp.Phys.Commn., arXiv:2503.22652)

R-ChFSI: Leveraging mixed precision compute

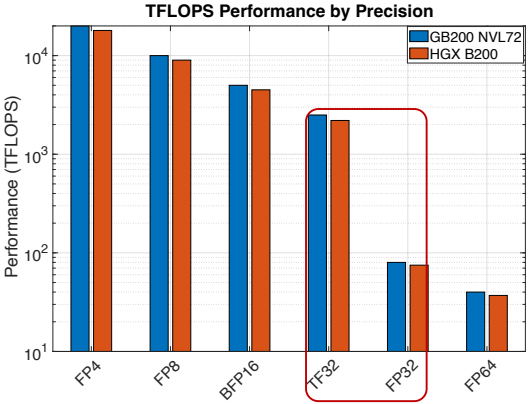

Lower precision compute in modern GPUs are orders of magnitude faster than `FP64`

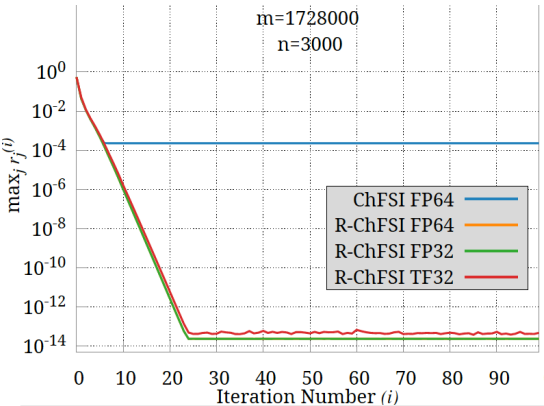

R-ChFSI is resilient to approximations in $T_m(\mathbf{S}^{-1}\mathbf{H})\boldsymbol{X}$: as the recurrence relation is in terms of **residuals**

$$\mathbf{Y}_{k+1}^{(i)} = \alpha \mathbf{H}\mathbf{S}_{apprx}^{-1}\mathbf{Y}_{k}^{(i)} + \beta \mathbf{Y}_{k}^{(i)} + \gamma \mathbf{Y}_{k-1}^{(i)}$$

Performance gains: Mixed precision compute

Benchmark system: Te deposited on WS_2 slab (10,000 electrons) with 6 Million DoFs
Computation performed on 120 GPUs of each super-computing system

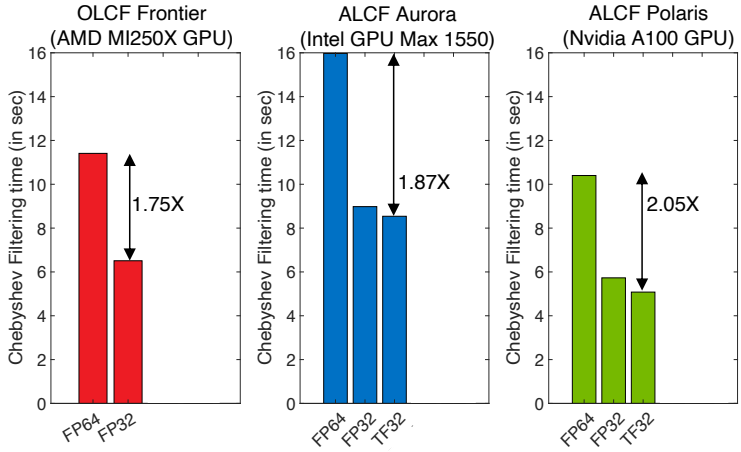

R-ChFSI: Leverage reduced precision MPI communication

Reduced precision communication across MPI tasks

- Every $\mathbf{HS}^{-1}\mathbf{X}$ requires inter-processor communications.
- Minimizing the data volume exchanged among MPI tasks directly decreases the total communication latency and bandwidth utilization.
- Conversion from FP32 to BF16 achieves $2\times$ reduction in P2P communication cost.

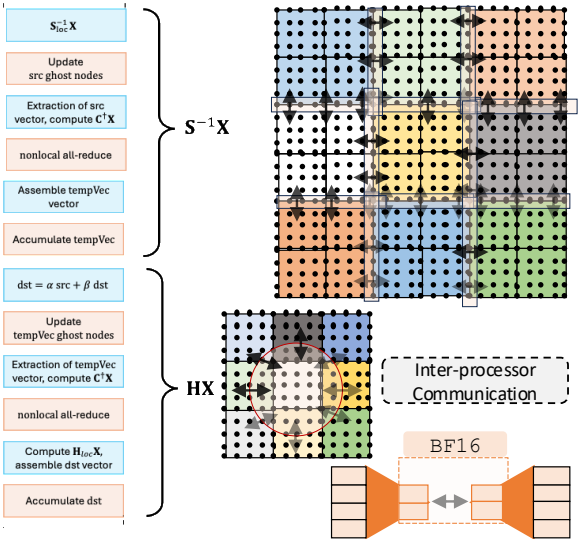

Performance gains: Reduced precision MPI communication

Benchmark system: Te deposited on WS_2 slab (10,000 electrons) with 6 Million DoFs
Computation performed on 120 GPUs of each super-computing system

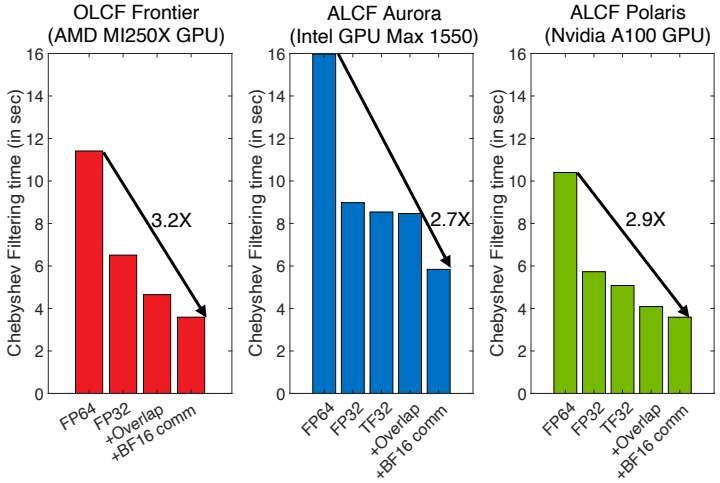

R-ChFSI: Leverage Block Floating Point Compressed Communication

Compressed communication across MPI tasks

- BF16 communication increases number of iterations certain cases; **fixed-rate BFP lossy compression preserves convergence**.
- Groups of 4 values share a common exponent and each encoded as signed coefficients.
- Supports arbitrary bits-per-value (BPV); optimized for BPV 8, 10, 12, and 16.
- FP32 → BPV12 reduces communication by 2.7× without degrading convergence; Can tolerate compression down to 8 BPV.

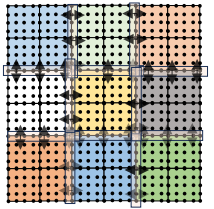

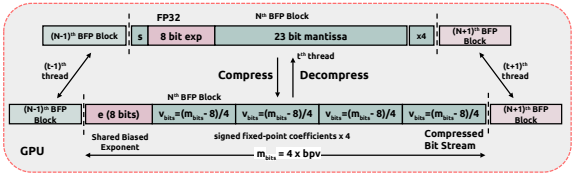

Strong scaling study

Pt_{2057} nanocluster

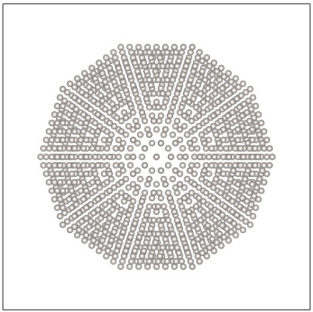

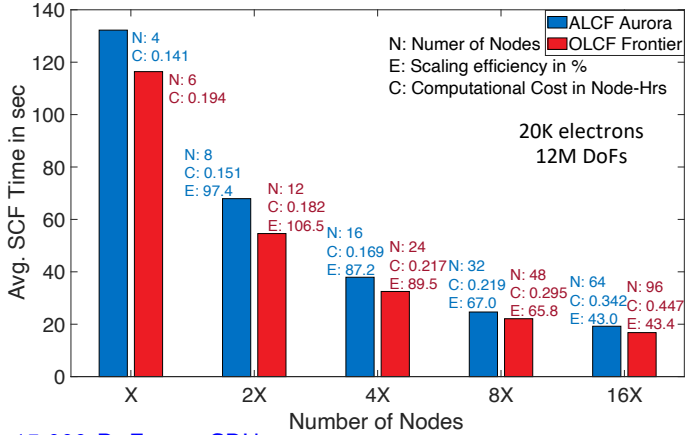

- Scaling efficiency is 43% even at 15,000 DoFs per GPU
- Energy error and force error with full precision is $\mathcal{O}(10^{-11})$ and $\mathcal{O}(10^{-8})$ respectively.
- A 100,000 electron system fits on 150 nodes (1800 GPUs) of ALCF Aurora (Intel GPUs) and takes less than 5 mins per SCF iteration!!

Key take aways

A few firsts...

- Proposed a subspace iteration strategy for large generalized eigenproblems accelerated by Chebyshev polynomial filters that is tolerant to errors in matrix-multivector multiplications.
- The eigensolver strategy can leverage approximations in inverse overlap matrix, reduced precision compute and further lower precision communication without loss of robustness
- Computationally efficient and robust eigensolver for solving large sparse generalized eigenproblem arising in finite-element discretized DFT using projector-augmented wave formalism.

Computational framework developed can enable realistic large-scale DFT calculations on latest heterogeneous computing architectures, impacting a diverse set of key scientific and technological areas, and opens up the door to numerous possibilities in materials design.

Giving back to community... DFT-FE (Open-source code)

$$\min_{\boldsymbol{\Psi}} \max_{\phi} E(\boldsymbol{\Psi}, \phi; \boldsymbol{R})$$

$$\boldsymbol{H}\boldsymbol{\psi}_i = \epsilon_i^h \boldsymbol{M}\boldsymbol{\psi}_i$$

Real-space DFT formulation & finite-element discretization

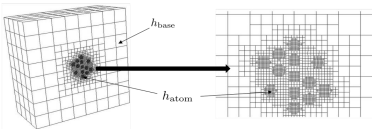

Adaptive higher-order (p >=5) spectral finite-elements

DFT-FE

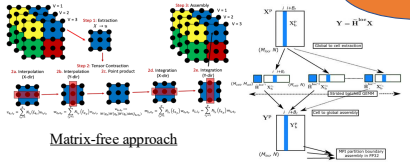

HPC-centric implementations

(1) **Unified framework** for all-electron and optimized norm-conserving Vanderbilt (ONCV) pseudopotentials.
(2) Fully periodic, semi-periodic and non-periodic boundary conditions with LDA, GGA, SCAN exchange-correlation functionals
(3) Large-scale **ONCV pseudopotential** DFT calculations demonstrated up to **600,000 electrons on 32,000 GPUs (43% of Peak on 8000 Frontier nodes)**

DFT-FE: https://github.com/dftfeDevelopers/dftfe

Workhorse behind ACM Gordon Bell Prize 2023 and ACM Gordon Bell Prize Finalist 2019

Development hubs at Univ. of Michigan and IISc

Acknowledgements

MATRIX Lab, IISc Bangalore

Nikhil (PhD) Kartick (PhD) Nishant (PhD) Gourab (PhD) Srinibas (PhD)

Collaborators:

- Mechanical and Materials Engineering , University of Michigan, Ann Arbor, USA
- Korean Institute of Science and Technology (KIST), South Korea
- Uppsala University, Sweden
- University of Tsukuba, Japan
- Research Institute for Sustainable Energy, T.C.G Crest, Kolkata
- Materials Engineering, Chemical Engineering, IISc Bangalore

Funding Agencies:

Relevant publications

1. N.Kodali, K. Ramakrishnan, P. Motamarri – Residual-based Chebyshev filtered subspace iteration for sparse Hermitian eigenvalue problems tolerant to inexact matrix-vector products, Computer Physics Communications, 2026

2. K. Ramakrishnan, P. Motamarri – Accelerating finite-element based projector-augmented wave density functional theory calculations with scalable GPU-centric computational methods (https://doi.org/10.48550/arXiv.2604.26037)

3. S. Das, B. Kanungo, V. Subramanian, G. Panigrahi, P. Motamarri, D M Rogers, P. Zimmerman, V. Gavini: Large-scale materials modeling at quantum accuracy: Ab initio simulations of quasicrystals and interacting extended defects in metallic alloys, Proceedings of SC23, (2023) [**Winning Team of 2023 ACM Gordon Bell Prize**]

Thank you!!!

Higher order FE basis

I. Cu nanoparticle
55 atoms

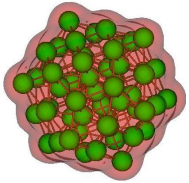

II. Mo periodic
supercell w/ vacancy
53 atoms

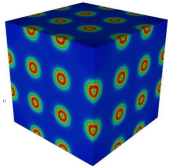

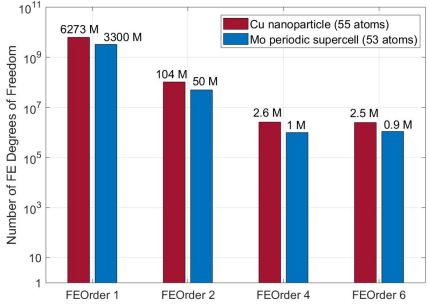

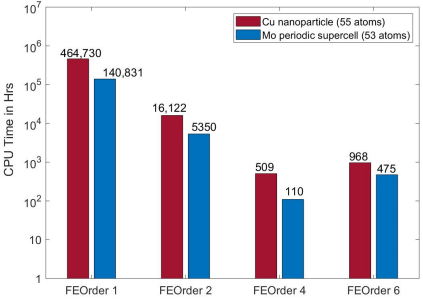

~1000x advantage by using higher-order FE basis !

Atomic forces in real-space DFT-FE:

- Ground-state energy for a fixed position of atoms:

$$E_0(\mathbf{R}) = \min_{\boldsymbol{\psi}} \max_{\varphi} \min_{\boldsymbol{\nu}_{\text{self}}} \Big[2 \sum_i \int_\Omega \psi_i^*(\mathbf{x}) \left(-\frac{1}{2}\nabla^2 \right) \psi_i(\mathbf{x})\, d\mathbf{x} + E_{xc}(\rho) + J(\rho, \varphi, \mathbf{R}) - E_{\text{self}}(\boldsymbol{\nu}_{\text{self}}, \mathbf{R}) \Big] \quad \text{subject to} \quad \int_\Omega \psi_i^*(\mathbf{x}) \psi_j(\mathbf{x})\, d\mathbf{x} = \delta_{ij}$$

- Using Hellmann-Feynman theorem, force acting on an atom I

$$\boldsymbol{f}_I = -\frac{\partial E_0}{\partial \mathbf{R}_I} = -Z_I \left[\nabla\varphi(\mathbf{R}_I) - \nabla\nu^I_{\text{self}}(\mathbf{R}_I) \right]$$

The above expression does not account for

- × FE basis-set error.
- × Elastic stress on a periodic unit-cell during any affine deformation.

Key Ideas in configurational force approach

(Motamarri & Gavini, Phys. Rev. B. 2018)

- Consider the perturbation of every material point $\mathbf{x}$ to $\mathbf{x}'$ via $\mathbf{x}' = \chi_\varepsilon(\mathbf{x}) = \mathbf{x} + \varepsilon\boldsymbol{\Upsilon}(\mathbf{x})$ with $\dfrac{d}{d\varepsilon}\chi_\varepsilon(\mathbf{x})\Big|_{\varepsilon=0} = \boldsymbol{\Upsilon}(\mathbf{x})$ and hence $\mathbf{J} = \dfrac{\partial \mathbf{x}'}{\partial \mathbf{x}}$.
- If $\mathcal{E}(\chi_\varepsilon)$ denotes the Kohn-Sham ground-state energy on the perturbed space, the configurational force is evaluateds by computing the Gateaux derivative of $\mathcal{E}(\chi_\varepsilon)$ i.e $\dfrac{d}{d\varepsilon}E(\chi_\varepsilon)\Big|_{\varepsilon=0}$.
- If the density matrix $\boldsymbol{\Gamma}^{\phi^\varepsilon}$, wavefunctions $\boldsymbol{\Phi}^\varepsilon = \{\phi_i^\varepsilon(\mathbf{x}')\}$, electrostatic potentials φ^ε and $\{V^{\varepsilon I}\}$ denote the solutions of the Kohn-Sham saddle point problem on the perturbed space, the Kohn-Sham energy functional with the constraint on the number of electrons:

$$\mathcal{E}(\chi_\varepsilon) = E_{\mathrm{KS}}^\varepsilon(\boldsymbol{\Gamma}^{\phi^\varepsilon}, \boldsymbol{\Phi}^\varepsilon, \varphi^\varepsilon, \{V^{\varepsilon I}\}) - E_{\mathrm{ent}}^\varepsilon - \mu\left[2\ tr(\boldsymbol{\Gamma}^{\phi^\varepsilon}) - N_e\right]$$

$$E_{\mathrm{KS}} = T_s^\varepsilon(\boldsymbol{\Gamma}^{\phi^\varepsilon}, \boldsymbol{\Phi}^\varepsilon) + \int_\Omega \epsilon_{xc}(\rho^\varepsilon)\rho^\varepsilon\ d\mathbf{x} + J^\varepsilon(\rho^\varepsilon, \mathbf{R}) - E_{\mathrm{self}}^\varepsilon(, \{V^{\varepsilon I}\})$$

Key Ideas in configurational force approach

- As an example, consider the term T_s in the perturbed space Ω'

$$T_s^{\varepsilon}(\,\chi_\varepsilon(\mathbf{x})\,) = 2\int_{\Omega'} \mathbf{\Gamma}_{ij}^{\phi^\varepsilon}\, {S_{jk}^{\varepsilon}}^{-1}\, \nabla_{\mathbf{x}'}\phi_k^{\varepsilon *}(\mathbf{x}')\nabla_{\mathbf{x}'}\phi_i^{\varepsilon}(\mathbf{x}')\, d\mathbf{x}'\,.$$

- Transforming the integrals back onto Ω in the above, we obtain

$$T_s^{\varepsilon} = 2\int_{\Omega} \mathbf{\Gamma}_{ij}^{\phi^\varepsilon}\, {S_{jk}^{\varepsilon}}^{-1}(\mathbf{\Phi}^{\varepsilon},\mathbf{J})(\mathbf{J}^{-1}\nabla_{\mathbf{x}}\phi_k^{\varepsilon *}(\,\chi_\varepsilon(\mathbf{x})\,))\cdot(\mathbf{J}^{-1}\nabla_{\mathbf{x}}\phi_i^{\varepsilon}(\,\chi_\varepsilon(\mathbf{x})\,))\det(\mathbf{J})\, d\mathbf{x}$$

- Similarly transforming all the other integrals in the Kohn-Sham functional back onto Ω, we then evaluate $\dfrac{d}{d\varepsilon}\mathcal{E}(\,\chi_\varepsilon(\mathbf{x})\,)\Big|_{\varepsilon=0}$.

$$\frac{d}{d\varepsilon}\mathcal{E}_c(\,\chi_\varepsilon(\mathbf{x})\,)\Big|_{\varepsilon=0} = \underbrace{T_f}_{\text{due to variations in fields}} + \underbrace{T_{\text{conf}}}_{\text{due to variations in space}}$$

- $T_f = 0$ as the electronic fields satisfy their E-L equations and T_{conf} can be written as

$$\frac{d}{d\varepsilon}\mathcal{E}_c(\,\chi_\varepsilon(\mathbf{x})\,)\Big|_{\varepsilon=0} = \int_{\Omega} \boldsymbol{E} : \nabla\mathbf{\Upsilon}(\mathbf{x})\, d\mathbf{x} + \sum_I \int_{\mathbb{R}^3} \boldsymbol{E}'^I : \nabla\mathbf{\Upsilon}(\mathbf{x})\, d\mathbf{x}$$

Numerical evaluation of forces and stresses

- To compute configurational forces in the FE setting, we discretize the generator $\boldsymbol{\Upsilon}(\mathbf{x})$ in the FE space spanned by the linear FE basis functions $\{\widetilde{N}_k(\mathbf{x})\}, k = 1 \cdots \widetilde{M}$ i.e $\Upsilon^h_j(\mathbf{x}) = \sum_i \Upsilon_{i,j} \widetilde{N}_i(\mathbf{x})$.
- Using $\Upsilon_{i,j} = 1$ for the i^{th} node and j^{th} direction, and $\Upsilon_{i,j} = 0$ otherwise, the force $\mathfrak{f}^h_{i,j}$ acting on the i^{th} node in the j^{th} direction can be computed using

$$\mathfrak{f}^h_{i,j} = \sum_{p=1}^{3} \left(\int_{\Omega} E^h_{jp} \, \frac{\partial \widetilde{N}_i(\mathbf{x})}{\partial x_p} \, d\mathbf{x} + \sum_I \int_{\mathbb{R}^3} E'^{hI}_{jp} \, \frac{\partial \widetilde{N}_i(\mathbf{x})}{\partial x_p} \, d\mathbf{x} \right), \, j = 1, 2, 3 \, ; i = 1 \cdots \widetilde{M} \, . \qquad (1)$$

- Forces on atomic nuclei are evaluated by choosing the appropriate generator $\boldsymbol{\Upsilon}^h$ compactly supported around the atom of interest.
- Stresses in periodic systems are evaluated by restricting the generator to affine deformations.

Numerical results: Variational nature of forces and stresses (Motamarri & Gavini, Phys. Rev. B. 2018)

Case study: SiF_4 and N_2

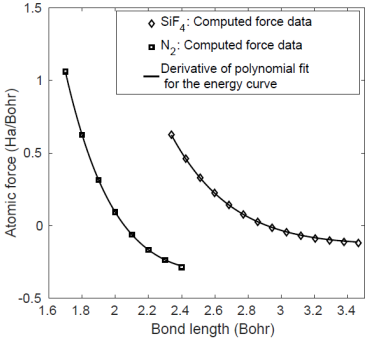

Case study: Al 3x3x3 Molecular Dynamics

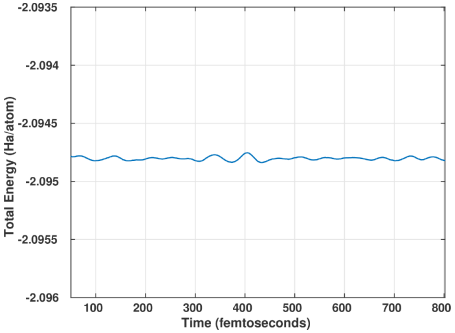

Geometry optimization of Tris (bipyridine) Ruthenium (TBR)

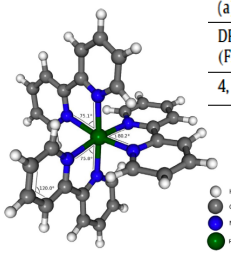

(a) Comparison of energies and forces in the un-relaxed TBR structure between DFT-FE and QE.

DFT-FE (FE_{ord}, h_{min}, h_{max})	DFT-FE E_g	DFT-FE f_{max}	QE E_{cut}	QE E_g	QE f_{max}
4, 0.42, 13.33	−5.5566947	0.1626628	50	−5.5566265	0.1626344

(b) Comparison between relaxed and un-relaxed TBR structures.

DFT-FE ΔE_{relax}	QE ΔE_{relax}
−0.0015992	−0.0016009